# S100A14 has AKT-mediated oncogenic potential and predicts poor prognosis in epithelial ovarian cancer

Hanbyoul Cho

Department of Medicine

The Graduate School, Yonsei University

# S100A14 has AKT-mediated oncogenic potential and predicts poor prognosis in epithelial ovarian cancer

Hanbyoul Cho

Department of Medicine

The Graduate School, Yonsei University

# S100A14 has AKT-mediated oncogenic potential and predicts poor prognosis in epithelial ovarian cancer

Directed by Professor Jae-Hoon Kim

The Doctoral Dissertation
submitted to the Department of Medicine,
the Graduate School of Yonsei University
in partial fulfillment of the requirements for the degree
of Doctor of Philosophy

Hanbyoul Cho

June 2013

This certifies that the Doctoral Dissertation of Hanbyoul Cho is approved.

---
Thesis Supervisor: Jae-Hoon Kim

---
[Thesis Committee Member#1: Yong Il Kwon]

---
[Thesis Committee Member#2: Jong-Hyeok Kim]

---
[Thesis Committee Member#3: Nam Hoon Cho]

---
[Thesis Committee Member#4: Jae Yong Cho]

The Graduate School
Yonsei University

June 2013

ACKNOWLEDGEMENTS

I would like to express profound gratitude to my supervisor, Professor Jae-Hoon Kim, for his invaluable support, encouragement, supervision and useful suggestions throughout this research work. His moral support and continuous guidance enabled me to complete my work successfully. I am also highly thankful to Professor Nam Hoon Cho, Jae Yong Cho, Jong-Hyeok Kim and Yong Il Kwon for their valuable suggestions throughout this study.

I would like to thank NIH (National Institute of Health) scientist, Joon-Yong Chung and our lab researcher, Ha-Yeon Shin for valuable advices in science discussion and guidance from the early stage of this research. Without their guidance and persistent help this thesis would not have been possible.

I am as ever, especially indebted to my parents for their love and support throughout my life. A special word of thanks is certainly in order for my beloved friend and wife, Dr. Ji In Chung, who assisted me with her encouragement and understanding during my study. Most especially, my thanks to

my dearly beloved children Erin Cho and Yesung Cho, you always had only new ways of supporting and encouraging me on, even during some difficult moments. This thesis is dedicated to my children Erin, Yesung and my wife Ji In. They have been my inspiration and motivation throughout this work.

Hanbyoul Cho

# <TABLE OF CONTENTS>

# LIST OF FIGURES

# LIST OF TABLES

<ABSTRACT>

# S100A14 has AKT-mediated oncogenic potential and predicts poor prognosis in epithelial ovarian cancer

Hanbyoul Cho

*Department of Medicine*
*The Graduate School, Yonsei University*

(Directed by Professor Jae-Hoon Kim)

**Purpose:** The purpose of this study was to identify genes and proteins those are highly differentially expressed in epithelial ovarian cancer (EOC), and to use this knowledge for the development of novel diagnostic and therapeutic markers for EOC. We further performed the validation and functional studies of S100A14, which was overexpressed in all of the six EOC cells by microarray analysis and has been implicated in tumorigenesis and metastasis.

**Materials and methods:** We have established 6 new EOC cell lines and characterized these via post genomics and post proteomics. To validate the results of the microarray, a total of 104 ovarian tissue specimens (13 normal ovarian tissues, 10 benign ovarian tumors, 10 borderline ovarian tumors, and 71 EOC tissues) were studied for S100A14 protein expression. Subsequently, we investigated the possible functions of S100A14 in EOC by lentivirus-mediated overexpression and short hairpin RNA (shRNA) approaches.

**Results:** Illumina microarray platform enabled us to identify 859 genes that were commonly up-regulated and 1116 genes that were down-regulated in EOC cell lines (> 2-fold, $P < 0.05$). In validation studies, *S100A14* mRNA expression was up-regulated in EOC cells by real-time PCR. Similarly, western blotting and IHC showed that S100A14 protein was significantly over-expressed in EOC cells and tissues. In addition, S100A14 expression was significantly associated

with advanced stage ($P$<0.001), serous type ($P$=0.004), and poor tumor grade ($P$<0.001). In multivariate analysis, S100A14 overexpression was the independent prognostic factor for overall (Hazard Ratio = 4.53 [1.16-17.69], $P$=0.029) and disease-free survival (Hazard Ratio = 3.10 [1.22-7.89], $P$=0.017). *In vitro* analysis of cell function revealed that the ectopic expression of S100A14 promoted cell proliferation, tumorigenesis, migration, and invasion through PI3K/Akt pathway, whereas S100A14 knockdown inhibited the effects of S100A14.

**Conclusions:** Taken together, these data show the aberrant expression of S100A14 in EOC and suggest a potential important role of S100A14 in ovarian carcinogenesis. This implies S100A14 could be used as a novel therapeutic target for ovarian cancer treatment.

---

Key words : epithelial ovarian cancer; tumor marker; S100A14; lentivirus; shRNA

# S100A14 has AKT-mediated oncogenic potential and predicts poor prognosis in epithelial ovarian cancer

Hanbyoul Cho

*Department of Medicine*
*The Graduate School, Yonsei University*

(Directed by Professor Jae-Hoon Kim)

## I. INTRODUCTION

Ovarian cancer is the leading cause of death from gynecological malignancies in developed countries.[1] Despite their clinical importance, little is known about the early stages in the development of these neoplasms, mainly because of the clinical inaccessibility of the ovaries, the frequent lack of symptoms until the tumors are disseminated, and the lack of adequate animal models. The most common form of cancer of the ovary is epithelial ovarian cancer (EOC). EOCs are believed to originate either from the normal ovarian surface epithelium itself or from its derivatives, the crypts and inclusion cysts on the surface epithelium.[2] Understanding the molecular basis of EOC may significantly refine the diagnosis and management of these tumors and may eventually lead to the development of novel, more specific and more effective treatment modalities.

S100 proteins, a large subgroup of EF-hand protein family, are small calcium-binding proteins which can function as both intra- and extracellular signaling molecules. They exert a broad range of intracellular and extracellular

functions through the modulation of their subcellular localization and interacting with specific target proteins, responsible for regulation of inflammation process, cell growth, cell motility, cell survival and apoptosis.[3-5] Expression of many of the S100 proteins has been reported to be altered in various human malignancies.[6] In addition, some S100 proteins, namely S100A2, S100A4, and S100P have been implicated in tumor invasion and metastasis.[7-9]

S100A14 is a recently identified member of the S100 calcium-binding proteins, whose biological function has not been clarified yet.[10] It is differentially expressed in a wide variety of cell types and is up-regulated in several tumors, such as ovary, lung, breast, and uterine tumors but down-regulated in certain types of tumors, such as kidney, colon, rectal, and esophageal tumors.[10] S100A14 may play vital roles in bladder tumorigenesis and progression.[11] In addition, S100A14 has also been reported to regulate oral squamous cell carcinoma cell invasion by modulating expression of MMP1 and MMP9.[12] However, the functional role of S100A14 protein in carcinogenesis and the underlying molecular mechanisms needs to be further investigated.

In this study, we first analyzed the gene expression patterns in 6 EOC cell lines (YDOV-13, YDOV-105, YDOV-139, YDOV-151, YDOV-157, and YDOV-161), which were newly established and characterized in our institute, and compared the gene expression to 4 human ovarian surface epithelial (HOSE) cells. We also compared the proteome of 3 EOC cell lines and 3 HOSE cells using two-dimensional gel electrophoresis (2-DE), matrix-assisted laser desorption/ionization time-of-flight (MALDI-TOF), and peptide mass fingerprinting (PMF) proteome analysis. Some of the identified genes are already known to be up-regulated in ovarian cancer, which further validate our experimental approach as well as our criteria for the determination of differentially expressed genes; but several genes represent novel findings. *S100A14*, which was one of the most up-regulated genes in our gene profiling, was validated through real-time PCR and immunohistochemical analysis. To

further elucidate the roles of S100A14 in ovarian carcinogenesis, we performed the functional study using lentivirus-mediated overexpression and short hairpin RNA (shRNA) approaches followed by various *in vitro* assays.

## II. MATERIALS AND METHODS

### 1. Cell lines and culture

All biosamples were obtained with appropriate informed consent from participants according to institutional review board (IRB) guidelines. Tumor samples were collected from surgeries or paracentesis performed at the Gangnam Severance Hospital, Yonsei University College of Medicine. Normal samples were obtained from tumor-free participants that had undergone surgery for benign pathology. Six EOC cell lines and 10 HOSE cells were established and characterized in this laboratory. Detailed culture procedures are described elsewhere.[13,14] SNU-840 was purchased from Korean Cell Line Bank (KCLB, Seoul, Korea) and SKOV3, TOV112D, OVCA429, OVCA433B, and RMUG-S cell lines from American Type Culture Collection (ATCC, Manassas, VA, USA), and maintained in DMEM/F12 supplemented with 10% FBS in the presence of 5% $CO_2$ at 37$^{o}$C in a humidified incubator. HOSE cells were cultured in 1:1 MCDB-105 and M199 supplemented with 10% FBS. YDOV-13, YDOV-105, YDOV-139, YDOV-151, YDOV-157, YDOV-161, TOV112D, OVCA429 and OVCA433B were cultured in Dulbecco's Minimal Eagle Medium (DMEM) supplemented with 10% FBS. SNU840 and SKOV3 were cultured in RPMI-1640 supplemented with 10% FBS. RMUG-S was cultured in Ham's F12 supplemented with 10% FBS. All cells were cultured at 37°C in 5% $CO_2$ atmosphere.

**2. RNA preparation and cDNA microarray**

Total RNA was extracted from 6 EOC cell lines and 4 HOSE cells using Trizol (Invitrogen Life Technologies, Carlsbad, CA, USA), and purified using RNeasy kit (Qiagen, Inc. Valencia, CA, USA) according to the manufacturers' suggested protocol. Biotinylated cRNA for hybridization was generated according to Illumina's recommended sample labeling procedure (Ambion, Inc., Austin, TX, USA) based on the industry standard single round Eberwine assay.[15] In brief, 500 ng total RNA was used for complementary DNA (cDNA) synthesis, followed by an amplification/labeling step (*in vitro* transcription) to synthesize biotin-labeled cRNA using the Ambion Illumina RNA amplification kit (Ambion, Inc.). The quality of total RNA was checked by gel analysis using the total RNA Nano chip assay on an Agilent 2100 Bioanalyzer (Agilent Technologies GmbH, Berlin, Germany). The cRNA was quantified using a NanoDrop® ND-1000 Spectrophotometer (NanoDrop Technologies, Wilmington, DE, USA). Chip hybridization, washing, Cy3-streptavidin (GE Healthcare, Amersham Biosciences, Uppsala, Sweden) staining, and scanning was performed on the Illumina BeadStation 500 platform (Illumina Inc., San Diego, CA, USA) employing reagents and protocols supplied by the manufacture. A total of 750 ng of labeled cRNA samples were hybridized as biological duplicates on Sentrix Human Ref-6-V2 Expression Bead Chip (Illumina Inc.). Arrays were scanned with Illumina BeadArray Reader confocal scanner (Illumina Inc.) according to the manufacturer's instructions.

**3. Gene expression data analysis**

A total of 24,957 probes were used in the final analysis. Array data processing and analysis were performed using BeadStudio software (Illumina

Inc.). The bead-averaged data was normalized using a quantile normalization method[16] and base-2 logarithmic (log2) transformed. The fold change was used to demonstrate rate of changes in average gene expressions between study groups. Statistical analyses were performed using the false discovery rate (FDR) with a significance threshold of 0.1. One-way analysis of variance (ANOVA) was used to determine differentially expressed sets of genes across the three experimental groups. Following analysis, 2520 genes were selected with the common conditions of: (1) *P* value of ANOVA < 0.05, (2) |Fold (Cancer/Normal)| > 2 and *P* value < 0.05. Statistical analyses of the data were performed with the Arrayassist® program (Stratagene, La Jolla, CA, USA).

**4. Two-dimensional gel electrophoresis (2-DE), image analysis, and identification of differential protein spots by MALDI-TOF/PMF**

The procedures of 2-DE and MALDI-TOF/PMF were the same as the previous study.[13]

**5. Patients and tumor specimens**

Seventy one EOC tissues (54 serous, 6 mucinous, 4 endometrioid, 2 transitional cell, 2 mixed, 2 clear cell, and 1 Brenner tumor), 9 borderline ovarian tumors (5 serous and 4 mucinous), 11 mucinous cystadenomas, and 10 normal ovary specimens provided by the Korea Gynecologic Cancer Bank through Bio & Medical Technology Development Program of the Ministry of Education, Science and Technology, Korea were included in the study. Tumor staging was performed according to the International Federation of Gynecology and Obstetrics (FIGO) classification. All FIGO Stage I/II ovarian cancer patients had pelvic and para-aortic lymph node dissection according to the National Comprehensive Cancer Network (NCCN) clinical practice guidelines.

Medical records were reviewed to collect data including age, surgical procedure, survival time, and survival status. Response to therapy was assessed according to Response Evaluation Criteria in Solid Tumors (RECIST; version 1.0) by spiral computed tomography.[17] Data on tumor grade and cell type were obtained from reviewing pathology reports.

**6. Immunohistochemistry (IHC)**

Immunohistochemical studies were performed using the avidin-biotin technique with DakoCytomation LSAB+ System-HRP (DakoCytomation, Glostrup, Denmark). Paraffin sections were deparaffinized in 2 changes of xylene, rehydrated in graded ethanol, and treated for 30 min with 3% $H_2O_2$ solution in methanol to block endogenous peroxidase. After blocking in 10% goat serum in TBS for 30 minutes, sections were incubated in a moist chamber with rabbit anti-Human S100A14 polyclonal antibody (Proteintech Group, Inc. Chicago, IL, USA) diluted 1:100 for 1 hr at room temperature, followed by incubation with biotinylated secondary antibody (DakoCytomation) for 1 hr. The reaction product was developed with DAB (3,3'-diaminobenzidine) chromogen solution (DakoCytomation). Sections were counterstained with hematoxylin and mounted in Paramount aqueous mounting medium (DakoCytomation). Representative photomicrographs were recorded using a digital camera (Nikon, Tokyo, Japan).

To evaluate immunohistochemical expression of S100A14, we applied a 4-grade scoring system corresponding to the sum of staining intensity (0 = negative; 1 = weak; 2 = moderate; 3 = strong) and the percentage of positive cells (0 = 0%; 1 = 1 – 25%; 2 = 26 – 50%; 3 = 51 – 100% positive cells), as described elsewhere.[18] Slides were scored in the absence of any clinical data, and the final immunostaining score was the average score of three observers.

**7. DNA constructs**

To generate pCDH/*S100A14*, cDNA encoding human *S100A14* was amplified from pOTB7 *S100A14* cDNA clone (MHS1011-60727, Open Biosystems, Waltham, MA,USA) using primer set 5'-TTC TAG AGC CAC CAT GGG ACA GTG TCG GTC AG-3' (forward) and 5'-TTG CGG CCG CTC AGT GCC CCC GGA CAG-3' (reverse). The amplified cDNA was cloned into NotI-HF/XbaI restriction sites of the pCDH-Promoter-MCS-EF1 Lentivector (System Biosciences, Mountain View, CA, USA).

**8. shRNA constructs**

pLKO.1 *S100A14* shRNA libraries were purchased from Open Biosystems. Of five lentiviral constructs tested, two with the best knock-down efficiency were used for the experiments presented here; the human *S100A14* sequence ATCACTGAATTCCTGAGCATC for shRNA #2 and TGGTGAAAGTTCTTGATGAGG for shRNA #5 was used. The Non-target shRNA control vector (SHC002) was purchased from Sigma (Sigma Aldrich, St. Louis, MO, USA).

**9. Establishment of stable cell lines.**

HEK293T cells were co-transfected with the lentiviral vector, packaging plasmid, and envelope plasmid. Virus supernatant was collected 48 hours and 72 hours after transfection. To establish stable cell line, TOV112D, YDOV-151, SNU840, and OVCA429 cells were infected with virus at a multiplicity of infection (MOI) of 2. Cells were changed to fresh media 24 hours after infection. To select for infected cells, cells were added 2 μg/mL puromycin to the media. Cells were changed to fresh puromycin-containing

media as every other day for 2 weeks. We used cloning cylinders (Millipore, Billerica, MA, USA) for harvesting cell colonies.

**10. Reagents**

AKT inhibitor MK-2206 was purchased from Sellect (Huston, TX) and PI3 kinase inhibitor wortmannin was purchased from Sigma Aldrich (St. Louis, MO). The stock solution of 10mM MK-2206 and 1mM wortmannin were dissolved in dimethyl sulfoxide (DMSO).

**11. Real-time polymerase chain reaction (PCR)**

Total RNA was extracted using an RNeasy Mini kit (Qiagen, Valencia, CA, USA). Next, a total of 2 μg RNA from each sample was reverse transcribed into cDNA by SuperScript $^{TM}$ III first – strand synthesis system (Invitrogen, Carlsbad, CA, USA) according to the manufacturer's suggested protocol. Real-time PCR was performed to quantify messenger RNA expressions using SYBR® Green PCR Master Mix (Applied Biosystems, Foster City, CA, USA) and the ABI PRISM® 7300 real-time PCR system (Applied Biosystems) according to the manufacturer's instructions. The thermal cycling conditions consisted of a pre-incubation for 2 min at 50$^{o}$C, then denaturation for 10 min at 95$^{o}$C followed by 40 cycles of denaturation for 15 sec at 95$^{o}$C and annealing/extension for 1 min at 60$^{o}$C. A housekeeping gene, glyceraldehyde-3-phosphate dehydrogenase (GAPDH), was used to normalize the quantity of cDNA used in the PCR reaction. Each assay was done in triplicate and expressed as the mean ± SD (standard deviation). A series of dilutions were prepared from a stock solution of total RNA to generate a standard curve to check the efficiencies of each reaction. The primers for the PCR analysis were as follows : for *S100A14* forward 5'-GTG TCG GTC AGC

CAA CGC AGA-3', *S100A14* reverse 5'-TGC TGG GTG ACC AGG TCC CGT-3', MMP1 forward 5'-CTG CTG CTG CTG TTC TGG GGT-3', MMP1 reverse 5'-CCA CTG GGC CAC TAT TTC TCC GCT-3', MMP2 forward 5'-GAT ACC CCT TTG ACG GTA AGG A -3', MMP2 reverse 5'CCT TCT CCC AAG GTC CAT AGC -3', MMP9 forward 5'- AGA CGG GTA TCC CTT CGA CG -3', MMP9 reverse 5'- AAA CCG AGT TGG AAC CAC GAC -3', GAPDH forward 5'- GAA GGT GAA GGT CGG AGT -3', GAPDH reverse 5'- GAA GAT GGT GAT GGG ATT TC -3'. The comparative $C_T$ method was used to calculate relative quantification of gene expression as described previously.[19]

**12. Western blotting**

Whole cell extraction was conducted using PRO-PRE Protein Extraction Solution (Intron Biotechnology, Seongnam, Korea). Equal amounts (20 μg) of each sample were separated on 8-15% SDS-PAGE and transferred to nitrocellulose membrane. The membranes were blocked with 5% nonfat dry milk in TBST (50 mM Tris, 150 mM NaCl, 0.1% Tween-20, pH 7.5) for 1 hour at room temperature, washed with TBST, and subsequently incubated with primary antibodies (anti-S100A14: Proteintech Group, Inc. Chicago, IL, Cat.#10489-1-AP, anti-Cyclin A: Cell Signaling Technology, Inc., Danvers, MA, USA, Cat.# 4138, anti-phospho-Akt(ser473): Cell Signaling Technology, Inc., Cat.# 4060 or anti-Akt (pan): Cell Signaling Technology, Inc., Cat.# 4691, anti-phospho-Erk1/2(Thr202/Tyr204) : Cell Signaling Technology, Inc., Cat.# 4511 or anti-Erk1/2 : Cell Signaling Technology, Inc., Cat.# 4695, anti-GAPDH: Santa Cruz Biotechnology, Santa Cruz, CA, USA, Cat.# sc-59541) in TBST overnight at 4°C. Primary antibodies against each protein were detected by secondary antibodies conjugated with horseradish peroxidase (GE Healthcare, Munich, Germany). Specific bands for each protein were detected on AGFA X-ray film (Agfa Health Care, Mortsel, Belgium) using the

SuperSignal Chemiluminescence kit (Thermo Scientific, Rockford, IL, USA).

**13. Cell proliferation assay**

Cell proliferation was measured by WST-1 assay (DaeilLab, Seoul, Korea). In brief, cells were seeded at $3x10^3$ viable cells/well on a 96-well microtiter plates in a final volume of 100 μL/well. Cells were incubated with WST-1 at 37°C for 2 hours and optical density (OD) values at 450 nm were recorded at days 0, 3, and 5 using a 96-well microplate reader (Bio-Rad Laboratories, Inc., Hercules, CA, USA). The experiment was performed in three replicates.

**14. Soft agar assay for colony formation**

Cells were seeded into 0.3% agar containing 10% FBS on top of a bed of 0.6% agar in 60-mm dishes at $3x10^3$ cells/well in a 60-mm dish. Plating was done in triplicates. After 1 week of incubation (37°C and 5% $CO_2$), approximately 1 mL of media was added to the dishes to avoid drying out and to ensure the cells had sufficient nutrients. Four weeks later, colonies were stained with 0.5% crystal violet and then stained colonies subsequently evaluated visually for the presence of colonies.

**15. Clonogenic assay (colony-forming assay)**

Cells were plated in a 60-mm dishe ($0.02\sim01\times10^4$ cells/well), and cultured for 3 weeks. Then the cells were fixed with 10% methanol and 10% acetic acid and stained with 0.5% crystal violet and then stained colonies subsequently evaluated visually for the presence of colonies.

**16. Wound healing Assay**

Cells were seeded at $1\times10^5$ cells/well in 12-well plates and then pre-incubated for 24 hours before creating a wound across the cell monolayer with a yellow plastic tip. Phase contrast images of the gaps were captured at baseline and after 24 hr with an inverted microscope (magnification, 10X).

**17. Matrigel invasion assay**

Cell invasion assays were performed with Neuro Probe 48-Well Micro Chemotaxis Chamber (Neuro Probe, Inc., Gaithersburg, MD) according to the manufacturer's instruction. In brief, cells ($0.5\times10^5$ viable cells/well) were seeded in the upper chamber, which was coated with Matrigel (BD Transduction Lab, San Jose, CA), and serum-free medium containing 0.1-10% FBS was added to the lower chamber. After 24 hour of incubation, non-migrating cells were removed from the upper chamber with a cotton swab and the cells present on the lower surface of the insert were stained with Differential Quik Stain Kit (Triangle Biomedical Sciences, Inc., Durham, NC). The number of invading cells was quantified by counting of least six random fields (total Magnification x200 per filter). The experiment was repeated three times.

**18. Statistical Analysis**

Normality distribution was assessed using the Shapiro-Wilk test. Because the distribution was not normal, univariate comparisons for quantitative variables between normal and cancer were made using non-parametric statistics (Kruskal–Wallis and Mann–Whitney U) where appropriate. Results with two-tailed *P* values less than 0.05 were considered statistically significant. Statistical analyses were performed using SPSS version

18.0 (SPSS Inc., Chicago, IL).

## III. RESULTS

### 1. Establishment and characterization of cell lines

A total of 6 EOC cell lines (YDOV-13, YDOV-105, YDOV-139, YDOV-151, YDOV-157, and YDOV-161) were established after sterile processing of surgical samples. General characteristics of cell lines are described in Table 1. YDOV-13 was derived from the patient with Brenner tumor and YDOV-151 was from mucinous tumor. Among the cell lines derived from serous tumor, YDOV-105 was from grade 2 tumor and YDOV-139, YDOV-157, and YDOV-161 was from grade 3 tumor. Sequencing of BRCA1/2 demonstrated several point and missense mutations in BRCA2. Wild-type sequences (215 G/G) were detected in exon 4 of the *p53* gene, except in one cell line (YDOV-13) with codon 215 C/C. The average population doubling time ranged from 19.0 hr to 133.3 hr. All cell lines were free of contamination by mycoplasma.

**Table 1. General characteristics of 6 newly established EOC cells.**

| | YDOV-13 | YDOV-105 | YDOV-139 | YDOV-151 | YDOV-157 | YDOV-161 |
|---|---|---|---|---|---|---|
| **<Characteristics of patients from whom cell lines were established>** | | | | | | |
| **Age** | 42 | 48 | 68 | 21 | 47 | 52 |
| **Stage (Initial)** | IIIc | IIIc | IIIc | Recurrent (Ic) | Recurrent (IIIc) | Recurrent (IIIc) |
| **Primary Tumor** | Brenner tumor | Serous type (Grade 2) | Serous type (Grade 3) | Mucinous type (Grade 3) | Serous type (Grade 3) | Serous type (Grade 3) |
| **Site** | Ascites | Ovary; tissue | Ascites | Ascites | Ascites | Ovary; tissue |
| **Chemotherapy** | Paclitaxel 175 mg/m$^2$ + Carboplatin (AUC6) | Paclitaxel 175 mg/m$^2$ + Carboplatin (AUC6) | Paclitaxel 175 mg/m$^2$ + Carboplatin (AUC4) | Docetaxel 75 mg/m$^2$ + Carboplatin (AUC4) | Paclitaxel 135 mg/m2 (IV) + Cisplatin 100 mg/m$^2$ (IP) + Paclitaxel 60 mg/m$^2$ (IP) | Etoposide 100 mg/m$^2$ + Carboplatin (AUC6) |
| **Response** | CR | CR | PR | PD | CR | PD |

**<Characteristics of newly established EOC cell lines>**

| | | | | | | |
|---|---|---|---|---|---|---|
| **Tumor marker** | | | | | | |
| CA125 (IU/mL) | 157.97 | 3639.1 | 2487.8 | 10.8 | 2.8 | 376.1 |
| CA19-9 (IU/mL) | < 0.1 | 3758.7 | 2476.6 | 0.11 | < 0.1 | < 0.1 |
| CA15-3 (IU/mL) | 0.4 | 11.2 | 13.1 | < 0.1 | < 0.1 | < 0.1 |
| CEA (ng/mL) | < 0.5 | 6.39 | 5.3 | < 0.5 | < 0.5 | < 0.5 |
| **Oncogene** | | | | | | |
| BRCA1 | normal | normal | normal | mutation | normal | mutation |
| BRCA2 | mutation | mutation | mutation | mutation | mutation | normal |
| p53 exon4 | codon 215 C/C (mutant) | 215 G/G (wild type) | 215 G/G (wild type) | 215 G/G (wild type) | 215 G/G (wild type) | codon 215 C/C (mutant) |
| **HLA ABC DNA typing** | | | | | | |
| A DNA typing | A*0201/A*2402 | A*24/A*31 | A*24/A*31 | A*38/A*38 | A*0207/A*0301 | A*1101/A*3101 |
| B DNA typing | B*4001/B*5201 | B*07/B*35 | B*07/B*35 | B*58/B*58 | B*4402/B*4601 | B*4403/B*5201 |
| C DNA typing | Cw*0401/ Cw0501 | Cw*03(09)/ Cw*07 | Cw*03(09)/ Cw*07 | Cw*03(10)/ Cw*03(Cw*10) | Cw*0102/ Cw*0501(3) | Cw*0702/ Cw*0801 |
| **HLA DR DNA typing** | DRB1*15/ DRB1*15 | DRB1*01/ DRB1*15 | DRB1*01/ DRB1*15 | DRB1*03/ DRB1*04 | DRB1*0803/ DRB1*1301 | DRB1*1410/ DRB1*1501 |
| **Doubling time (hours)** | 38.4 | 133.3 | 120.0 | 19.0 | 102.0 | - |
| **Chemosensitivity** | ok | ok | ok | ok | ok | ok |
| **Tumorigenicity** | moderate (++) | weak (+) | weak (+) | weak (+) | weak (+) | - |

## 2. Gene expression profiling

Comprehensive gene expression profiles of 6 EOC cell lines (YDOV-13, YDOV-105, YDOV-139, YDOV-151, YDOV-157, and YDOV-161) and 4 HOSE cells (HOSE 198, 209, 211, and 213) were generated using a cDNA microarray with 24,957 probe sets. Hierarchical cluster analysis revealed that approximately 1975 genes were differentially expressed between EOC cell lines and HOSE cells (> 2-fold, $P < 0.05$) (Fig. 1A). Of the genes classified as having altered expression, 859 genes were up-regulated and 1116 genes were down-regulated in ovarian cancer. Using Gene Ontology classifiers, we group the genes with remarkable fold changes (> 2-fold) to investigate the association between these differentially expressed genes and functional pathways of ovarian cancer. A partial list of genes that were grouped into the different functional groups is presented in Table 2.

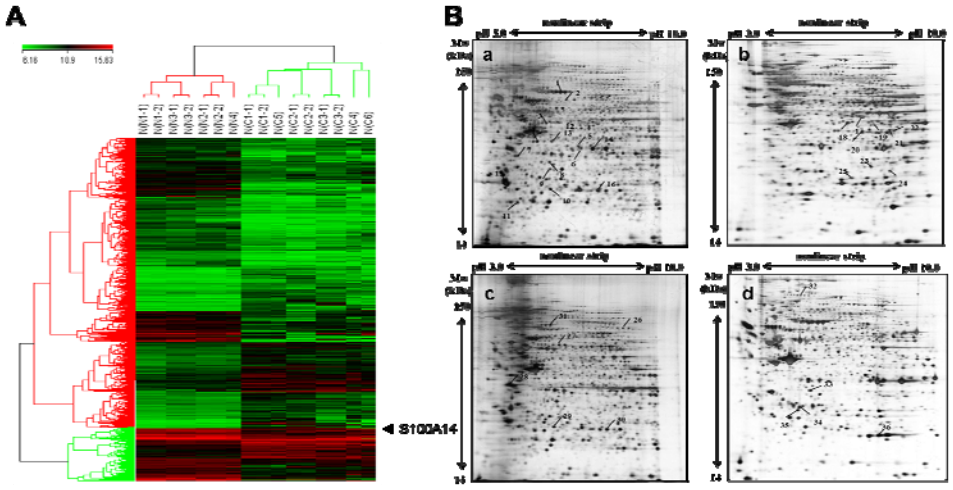


**Figure 1. Discovery of new biomarkers for EOC by microarray and 2-DE.**
A) Hierarchical clustering of 6 EOC cell lines and 4 HOSE cells. The dendrogram resulted from unsupervised cluster analysis that differentiated EOC from HOSE by gene expression profiling. Each column represents a sample. N: normal ovarian surface epithelial cells. C: cancer cells. B) Proteomic comparison between the a) YDOV-105, b) YDOV-157, c) YDOV-161, and d) HOSE 198 using 2-DE and MALDI-TOF/PMF. A total of 100 μg of total protein extract was loaded on pH3-10NL strips followed by 10% SDS-PAGE and silver staining. Black lines indicate identified protein spots significantly altered in EOC cell lines as compared to HOSE cell. Corresponding identifications are listed in Table 3.

**Table 2. Selected groups of differentially expressed genes between 6 EOC cells and 4 HOSE cells.**

| TargetID | Definition | Symbol | Fold† | Ontology |
|---|---|---|---|---|
| **<Up-regulated genes in 6 EOC cell lines>** | | | | |
| ILMN_21141 | huntingtin interacting protein 1 | HIP1 | **2.57** | apoptosis |
| ILMN_17182 | S100 calcium binding protein A14 | S100A14 | **6.29** | calcium ion binding |
| ILMN_8896 | S100 calcium binding protein A4 | S100A4 | **20.22** | calcium ion binding |
| ILMN_23486 | SNF1-like kinase | SNF1LK | **4.21** | cell differentiation |

| | | | | |
|---|---|---|---|---|
| ILMN_11560 | kallikrein 6 (neurosin, zyme) | KLK6 | **15.22** | cell differentiation |
| ILMN_11067 | pituitary tumor-transforming 1 | PTTG1 | **5.09** | cell division |
| ILMN_15254 | cyclin B2 | CCNB2 | **2.40** | cell division |
| ILMN_16427 | cyclin A2 | CCNA2 | **2.79** | cell division |
| ILMN_6835 | laminin, alpha 3 | LAMA3 | **8.36** | cell migration |
| ILMN_7052 | tetraspanin 1 | TSPAN1 | **6.33** | cell proliferation |
| ILMN_12370 | stratifin | SFN | **11.51** | cell proliferation |
| ILMN_30018 | transforming growth factor, alpha | TGFA | **4.62** | cell proliferation |
| ILMN_21302 | bone marrow stromal cell antigen 2 | BST2 | **16.49** | cell proliferation |
| ILMN_25097 | epithelial membrane protein 1 | EMP1 | **3.96** | cell proliferation |
| ILMN_25969 | kinesin family member 2C | KIF2C | **4.98** | cell proliferation |
| ILMN_21715 | lysosomal-associated membrane protein 3 | LAMP3 | **6.28** | cell proliferation |
| ILMN_10614 | wingless-type MMTV integration site family, member 7A | WNT7A | **6.61** | cell signaling |
| ILMN_9313 | fibroblast growth factor binding protein 1 | FGFBP1 | **4.40** | cell signaling |
| ILMN_25646 | S100 calcium binding protein A9 (calgranulin B) | S100A9 | **3.43** | cell signaling |
| ILMN_10988 | claudin 3 | CLDN3 | **18.54** | cell-cell adhesion |
| ILMN_13755 | claudin 7 | CLDN7 | **29.11** | cell-cell adhesion |
| ILMN_9707 | intercellular adhesion molecule 3 | ICAM3 | **2.37** | cell-cell adhesion |
| ILMN_19846 | mucin 1, transmembrane | MUC1 | **6.87** | cytoskeleton |
| ILMN_5566 | keratin 17 | KRT17 | **10.08** | epidermis development |
| ILMN_9653 | kallikrein 7 | KLK7 | **8.45** | epidermis development |
| ILMN_421 | solute carrier family 2, member 1 | SLC2A1 | **6.35** | glucose transport |
| ILMN_28723 | CD24 antigen (small cell lung carcinoma cluster 4 antigen) | CD24 | **4.41** | immune response |
| ILMN_18898 | mucin 20 | MUC20 | **5.27** | integral to membrane |
| ILMN_4070 | tumor-associated calcium signal transducer 1 | TACSTD1 | **62.01** | integral to membrane |
| ILMN_3183 | solute carrier organic anion transporter family, member 4A1 | SLCO4A1 | **33.33** | ion transport |
| ILMN_29459 | translocase of outer mitochondrial membrane 40 homolog | TOM40 | **2.55** | mitochondrial transport |
| ILMN_14210 | protease, serine, 8 (prostasin) | PRSS8 | **17.12** | proteolysis |
| ILMN_21619 | kallikrein 8 (neuropsin/ovasin) | KLK8 | **3.07** | proteolysis |
| ILMN_18118 | KIAA1815 | KIAA1815 | **3.97** | proteolysis |
| ILMN_18063 | nucleoside phosphorylase | NP | **3.47** | purine metabolism |
| ILMN_19881 | inositol(myo)-1(or 4)-monophosphatase 2 | IMPA2 | **11.42** | signal transduction |
| ILMN_5602 | keratin 23 (histone deacetylase inducible) | KRT23 | **3.15** | structural molecule |
| ILMN_19730 | E2F transcription factor 2 | E2F2 | **5.99** | transcription |

| | | | | |
|---|---|---|---|---|
| ILMN_13615 | E74-like factor 3 | ELF3 | **7.40** | transcription |
| ILMN_11468 | RAB25, member RAS oncogene family | RAB25 | **13.00** | transcription |
| ILMN_16252 | cellular retinoic acid binding protein 2 | CRABP2 | **11.48** | transcription |
| ILMN_20794 | lipocalin 2 (oncogene 24p3) | LCN2 | **64.70** | transport |
| **<Down-regulated genes in 6 EOC cell lines>** | | | | |
| ILMN_5665 | gap junction protein, alpha 1, 43kDa (connexin 43) | GJA1 | **-23.55** | cell-cell signaling |
| ILMN_14624 | wingless-type MMTV integration site family, member 5A | WNT5A | **-6.39** | cell-cell signaling |
| ILMN_24617 | FAT tumor suppressor homolog 1 (Drosophila) | FAT | **-5.40** | cell-cell signaling |
| ILMN_1037 | unc-13 homolog B (C. elegans) | UNC13B | **-2.18** | apoptosis |
| ILMN_28768 | death-associated protein kinase 3 | DAPK3 | **-3.27** | apoptosis |
| ILMN_2007 | tumor protein p53 inducible protein 3 | TP53I3 | **-2.11** | apoptosis |
| ILMN_20483 | glycoprotein (transmembrane) nmb | GPNMB | **-11.25** | cell proliferation |
| ILMN_14995 | fibroblast activation protein, alpha | FAP | **-15.54** | proteolysis |
| ILMN_14685 | zinc finger homeobox 1b | ZFHX1B | **-6.43** | transcription |
| ILMN_14655 | musculin (activated B-cell factor-1) | MSC | **-6.53** | transcription |
| ILMN_16131 | homeobox A5 | HOXA5 | **-21.53** | transcription |
| ILMN_5682 | complement component 3 | C3 | **-11.84** | signal transduction |
| ILMN_137280 | protein tyrosine phosphatase-like, member A | PTPLA | **-6.00** | signal transduction |
| ILMN_15406 | phosphoinositide-3-kinase, catalytic, delta polypeptide | PIK3CD | **-7.57** | signal transduction |
| ILMN_6876 | contactin associated protein 1 | CNTNAP1 | **-7.06** | signal transduction |

† 6 EOC cell lines/ 4 HOSE cells

Several genes involved in epidermis development and cell-cell adhesion were differently expressed in ovarian cancer, including *keratin 17*, *claudin 3*, *claudin 7*, and *intercellular adhesion molecule 3 (ICAM3)*. We identified a number of overexpressed genes associated with cellular process of carcinogenesis, including apoptosis, cell division, cell proliferation, and cell signaling. These genes include *huntingtin interacting protein 1 (HIP1)*, *cyclin A2/B2*, *tetraspanin 1*, *stratifin*, *bone marrow stromal cell antigen 2 (BST2)*, and *S100 calcium binding protein A9 (calgranulin B) (S100A9)*. A number of

oncogenes, including *pituitary tumor-transforming 1 (PTTG1)* and *E74-like factor 3 (ELF3)*, were identified in our analysis. We also identified a number of overexpressed genes previously associated with various cancers, including *tumor-associated calcium signal transducer 1 (TACSTD1) (Ep-CAM)*, *protease, serine, 8 (PRSS8) (prostasin)*, *mucin 20 (MUC20)*, *S100 calcium binding protein family (S100A4*, *S100A14)*, and *kallikreins (kallikrein 6, 7,* and *8)*.

### 3. 2-DE MALDI-TOF/PMF proteome analysis

Protein profiles from 3 EOC cell lines (YDOV-105, YDOV-157, and YDOV-161) and 1 HOSE cell (HOSE 198) were analyzed by 2-DE MALDI-TOF/PMF. A number of spots were found to be significantly altered ($P < 0.05$) or absent/emergent in EOC cell lines compared to HOSE cells and 31 up-regulated and 5 down-regulated spots were identified (Fig. 1B). Table 3 lists the proteins that were identified by MALDI-TOF and PMF.

**Table 3. Identification of proteins that were differentially expressed in 3 EOC cells compared to HOSE cells using 2-DE and MALDI-TOF/PMF.**

| Spot No. | Identification | % coverage | *pI*† | Mw (kDa) |
|---|---|---|---|---|
| **<Up-regulated proteins in EOC cell lines>** | | | | |
| 1 | Helicase-MOI | 9 | 5.5 | 221.53 |
| 2 | t-complex polypeptide 1 | 17 | 6.0 | 60.89 |
| 3 | Guanine deaminase | 20 | 5.2 | 44.51 |
| 4 | Thioredoxin-like protein | 30 | 5.2 | 37.76 |
| 5 | Enolase 1 | 29 | 7.0 | 47.49 |
| 6 | Protein phosphatase 1, catalytic subunit | 30 | 5.8 | 37.95 |
| 7 | Eukaryotic translation elongation factor 1 delta isoform 2 | 30 | 4.9 | 31.22 |
| 8 | Pyrophosphatase 1 | 42 | 5.5 | 33.10 |
| 9 | Annexin A4 | 37 | 5.8 | 36.09 |
| 10 | Heat shock protein 27 | 26 | 8.1 | 22.42 |
| 11 | Glyoxalase I | 27 | 5.1 | 20.99 |
| 12 | Ubiquinol-cytochrome c reductase core I protein | 11 | 5.9 | 53.29 |

| | | | | |
|---|---|---|---|---|
| 13 | PAP-inositol-1,4-phosphatase | 31 | 5.5 | 33.75 |
| 14 | Annexin 1 | 30 | 6.6 | 38.92 |
| 15 | YWHAZ protein | 20 | 7.0 | 35.55 |
| 16 | Peroxiredoxin 6 | 23 | 6.0 | 25.13 |
| 17 | EEF1G protein | 24 | 6.1 | 41.27 |
| 18 | S-adenosylhomocysteine hydrolase | 27 | 6.0 | 48.27 |
| 19 | Hypothetical protein | 22 | 6.4 | 42.64 |
| 20 | Tissue specific transplantation antigen P35B | 21 | 6.1 | 36.10 |
| 21 | Aspartate aminotransferase 1 | 45 | 6.5 | 46.46 |
| 22 | TOM40 protein | 17 | 6.8 | 34.71 |
| 23 | NP (nucleoside phosphorylase) | 31 | 6.5 | 32.33 |
| 24 | 5'-methythioadenosine phosphorylase | 32 | 6.8 | 31.73 |
| 25 | HP protein | 18 | 6.1 | 25.73 |
| 26 | MTHSP75 | 11 | 6.0 | 74.05 |
| 27 | ER-60 protein | 11 | 5.9 | 57.16 |
| 28 | Cytokeratin 9 | 46 | 5.1 | 62.27 |
| 29 | Heat shock protein 27 | 22 | 8.1 | 22.42 |
| 30 | Keratin 1 | 18 | 8.3 | 66.22 |
| 31 | SEC61A2 protein | 11 | 9.2 | 46.60 |
| **<Down-regulated proteins in EOC cell lines>** | | | | |
| 32 | VLA-3 alpha subunit | 7 | 6.1 | 114.5 |
| 33 | Annexin A3 | 53 | 5.6 | 36.53 |
| 34 | Chloride intracellular channel 4 | 60 | 5.5 | 28.98 |
| 35 | Nicotinamide N-methyltransferase | 23 | 5.6 | 30.01 |
| 36 | Manganese-containing superoxide dismutase | 36 | 6.9 | 23.77 |

Mw, molecular weights. † isoelectric value.

## 4. Validation studies using real-time PCR and IHC

Because of the abundance of S100A14 seen in microarray analysis of 6 EOC cells (Table 4) we focused our subsequent studies on this protein. To rule out the possibility that *S100A14* gene expression only occurs in newly established EOC cells during *in vitro* culture, we next performed the validation studies using PCR and IHC in various EOC cells and tissues. Reverse transcriptase-PCR (RT-PCR) and real-time PCR revealed that *S100A14* mRNA

levels is abundantly expressed in ovarian cancer cells excluding TOV112D, YDOV-151, and OVCA433B. However, *S100A14* expression was almost undetectable in HOSE cells. Lysate from HEK293T cell transfected with a pCDH/*S100A14* plasmid (lane designated as overexpress) was loaded as a positive control of RT-PCR and real-time PCR (Fig. 2A). In immunoblotting, we found that S100A14 is highly expressed in SNU840, YDOV-139, YDOV-105 cells, but it was not detected in HOSE cells (Fig. 2B). These observations suggest that expression of S100A14 protein occurs mostly in fully transformed cells.

**Table 4. Clinical information and cDNA microarray analysis for the 6 EOC cells.**

| Cell lines | Histology | Stage (Initial) | Grade | Sites | Age (years) | Microarray result (*S100A14* expression†) |
|---|---|---|---|---|---|---|
| YDOV-13 | Brenner | IIIc | - | Ascites | 42 | 7.29 |
| YDOV-105 | Serous | IIIc | II | Tissue | 48 | 9.85 |
| YDOV-139 | Serous | IIIc | III | Ascites | 68 | 5.37 |
| YDOV-151 | Mucinous | Recurrent (Ic) | III | Ascites | 21 | 7.82 |
| YDOV-157 | Serous | Recurrent (IIIc) | III | Ascites | 47 | 11.72 |
| YDOV-161 | Serous | Recurrent (IIIc) | III | Tissue | 52 | 1.12 |

†EOC cell line/4 HOSE cells

To determine whether S100A14 overexpression is linked to clinicopathological features of EOC, we performed IHC analysis of S100A14 protein in 104 ovarian tissue specimens. Most immunoreactivity was observed in the cytoplasm of tumor cells (Fig. 2C). Scoring results from the IHC analyses are summarized in Table 5. EOC tissues had greater S100A14 expression levels than in borderline tumor, benign tumor, or normal ovary tissues ($P<0.001$). Furthermore, S100A14 immunoreactivity significantly correlated with features associated with advanced disease and poor outcome including tumor stages

($P$<0.001), cell types ($P$=0.004), and tumor grades ($P$<0.001), with advanced stage, serous cell type, poor differentiation cases having higher IHC scores (Table 5, Fig. 2D).

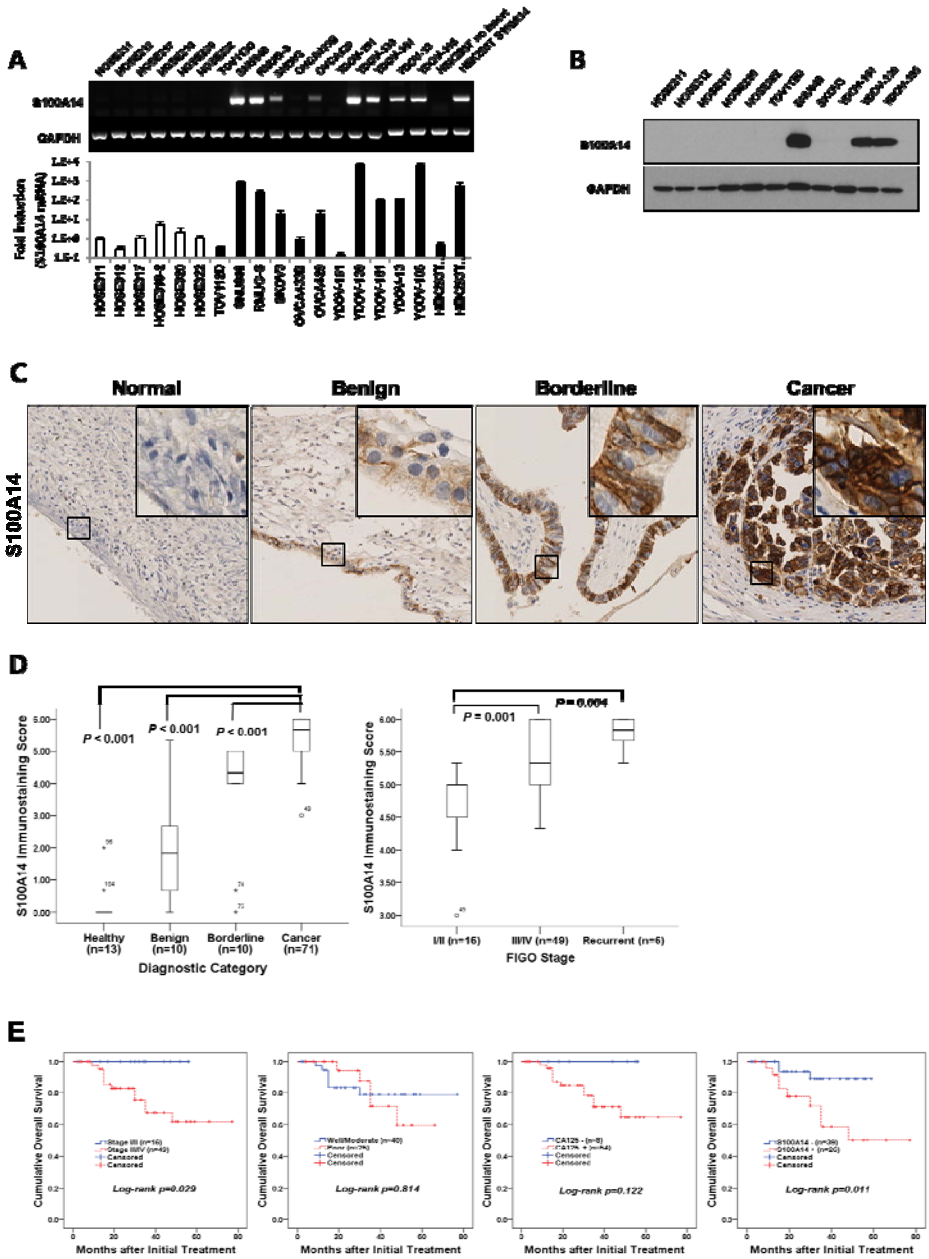

**Figure 2. S100A14 is highly expressed in human ovarian cancer cells and tissue specimens and its expression correlates with tumor stage and outcome of disease.**

A) *S100A14* mRNA levels were assessed by using RT-PCR (upper panel) and real-time PCR (lower panel) in the human ovarian surface epithelial (HOSE) cells and ovarian cancer cells. Expression of GAPDH was included as internal loading control. The Kruskal-Wallis analysis of variance and a post hoc Dunn method revealed statistically significant differences between EOC cell lines and HOSE cells ($P$ = 0.019). Each value is expressed as the mean of triplicate samples. The reference cell, HOSE 311, was considered to have a value of 1. B) S100A14 protein levels were analyzed by western blot. GAPDH was included as an internal loading control. C) Representative immunohistochemical staining for S100A14 in formalin-fixed paraffin-embedded EOC tissues (x400). D) IHC staining score of S100A14 in EOC samples was significantly higher than that in healthy controls, benign ovarian tumors, or borderline ovarian tumors ($P$ < 0.001). E) Kaplan-Meier plots for patients with epithelial ovarian cancer stratified according to FIGO stage, tumor grade, CA125 expression, or S100A14 expression.

**Table 5. S100A14 immunohistochemical staining score in EOC.**

| | No. of patients | Scores | | |
|---|---|---|---|---|
| | | **Geometric mean (95% CI)** | **Range** | ***P* value** |
| **Diagnostic category** | | | | **< 0.001** |
| Healthy | 13 | 0.20 (-0.13-0.54) | 0.0-2.0 | |
| Benign | 10 | 1.90 (0.70-3.10) | 0.0-5.3 | |
| Borderline | 10 | 3.76 (2.44-5.09) | 0.0-5.0 | |
| Cancer | 71 | 5.37 (5.21-5.52) | 3.0-6.0 | |
| **FIGO stage** | | | | **< 0.001** |
| I/II | 16 | 4.72 (4.40-5.05) | 3.0-5.3 | |
| III/IV | 49 | 5.51 (5.36-5.67) | 4.3-6.0 | |
| Recurrent | 6 | 5.89 (5.71-6.06) | 5.6-6.0 | |

| | | | | |
|---|---|---|---|---|
| **Cell type** | | | | **0.004** |
| Serous | 54 | 5.49 (5.32-5.66) | 3.0-6.0 | |
| Non-serous | 17 | 4.98 (4.71-5.24) | 4.0-6.0 | |
| **Tumor grade** | | | | **< 0.001** |
| Borderline | 10 | 3.76 (2.44-5.09) | 0.0-5.0 | |
| Well | 8 | 4.70 (3.94-5.47) | 3.0-6.0 | |
| Moderate | 33 | 5.30 (5.11-5.49) | 4.0-6.0 | |
| Poor | 30 | 5.62 (5.41-5.82) | 4.0-6.0 | |

CI, confidence interval; FIGO, International Federation of Gynecology and Obstetrics.

### 5. Prognostic significance of S100A14 expression

We next examined the relationship between S100A14 expression and prognostic outcome. Clinicopathological and outcome information were available for all of 65 EOC patients who were monitored for survival and recurrence; 6 recurrent EOC patients were excluded from the survival analysis. The follow up period of EOC ranged from 5 to 77 months, with a mean of 30.8 months. Twelve patients (18.4%) died within this period, 25 (38.5%) survived but suffered recurrence or persistent disease and 28 (43.1%) showed no evidence of disease after treatment. In the recurrent disease group (n = 24), the mean time to recurrence after initial treatment was 19.9 months.

Kaplan-Meier plots demonstrated that patients with advanced stage (III/IV) and S100A14+ (IHC score of > 5) displayed significantly worse overall survival ($P$=0.029 and $P$=0.011, respectively) (Fig. 2E). A Cox multivariate proportional hazards analysis showed that advanced stage (hazard ratio [HR] = 3.25, $P$=0.038 and HR = 4.31, $P$=0.024, respectively) and S100A14+ (HR = 3.10, $P$=0.017 and HR = 4.53, $P$=0.029, respectively) were independent prognostic factors with respect to both disease-free and overall survival (Table 6).

**Table 6. Univariate and multivariate analyses of the associations between prognostic variables and disease-free (DFS) and overall survival (OS) in EOC patients.**

| | DFS hazard ratio (95% CI[†]), *P* value | | OS hazard ratio (95% CI), *P* value | |
|---|---|---|---|---|
| | Univariate | Multivariate | Univariate | Multivariate |
| FIGO stage (III/IV) | 4.78 [1.86-12.23], *P*=0.001 | 3.25 [1.07-9.92], *P*=0.038 | 4.84 [1.62-14.48], *P*=0.005 | 4.31 [1.20-15.44], *P*=0.024 |
| Tumor grade (poor) | 2.49 [1.11-5.59], *P*=0.026 | 1.03 [0.43-2.46], *P*=0.938 | NS | NA |
| Cell type (Serous) | 4.49 [1.33-15.11], *P*=0.015 | 1.40 [0.36-6.41], *P*=0.665 | NS | NA |
| CA125+[†] | NS | NA | NS | NA |
| S100A14+[‡] | 6.74 [2.82-16.07], *P*=0.001 | 3.10 [1.22-7.89], *P*=0.017 | 6.42 [1.40-29.34], *P*=0.016 | 4.53 [1.16-17.69], *P*=0.029 |

CI, confidence interval; NS, not significant; NA, not applicable, CA125+[†] (> 35 U $ml^{-1}$), S100A14+[‡] (IHC score > 5).

**6. Establishment of stable cells by lentivirus**

As the biological function of S100A14 in EOC is largely unknown, we set out to investigate the potential role of S100A14 in the development of malignant phenotype by modulating intracellular S100A14 expression in EOC cells. We first established S100A14-overexpressed and knockdown stable EOC cells. For *S100A14*-overexpressed experiments, we selected TOV112D and YDOV-151 cells with low level of endogenous S100A14 expression. Conversely, we selected SNU840 and OVCA429 cells with high level of endogenous S100A14 for S100A14 knock-down experiments. Determination of S100A14 immunoreactivity indicated a high enrichment of S100A14 in TOV112D (*S100A14* #6, #8) and YDOV-151 (*S100A14* #6, #10) cells compared

with empty vector-expressed cells. The mRNA expression of *S100A14* was showed as the same results to western blotting (Fig. 3A). In contrast, the protein expression of S100A14 decreased by short-hairpin *S100A14* RNAi in SNU840 (sh-*S100A14* #2, #5) and OVCA429 (sh-*S100A14* #2, #5) cells (Fig. 3B). Finally, two most effectively overexpressed or knockdown constructs for each cell were further selected to investigate the phenotypical change due to S100A14 up- or down-regulation.

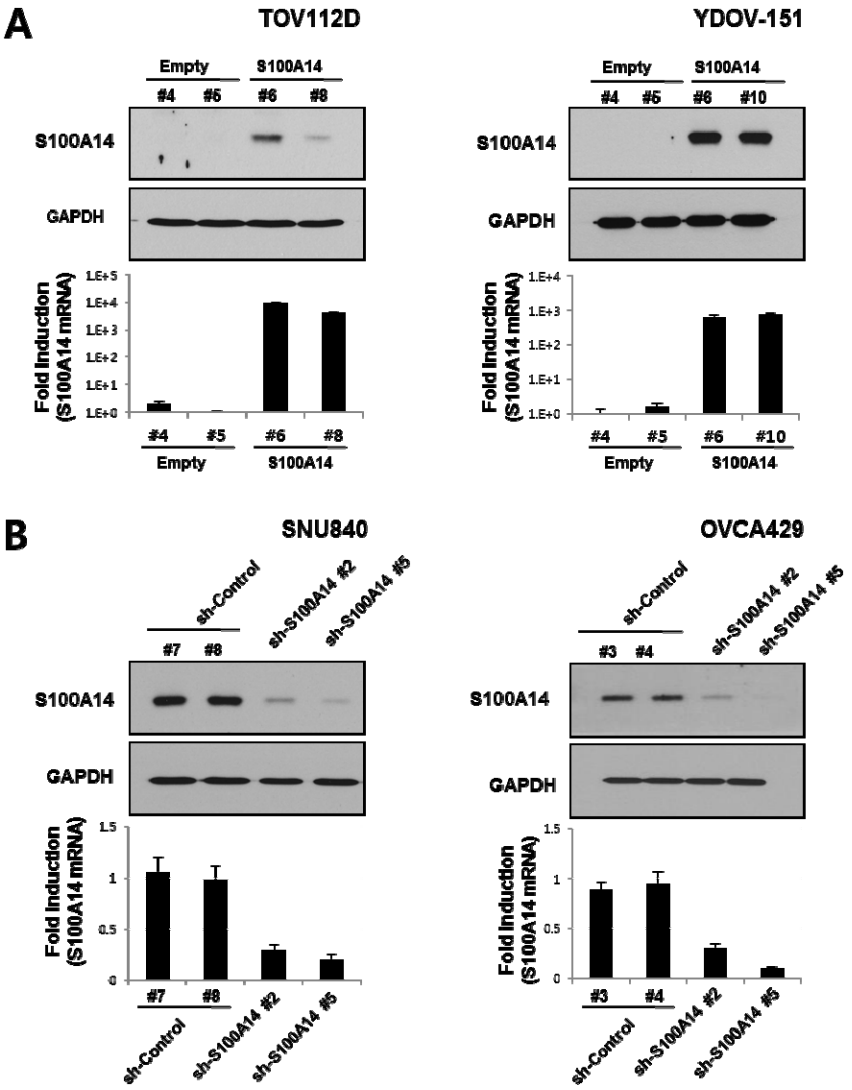

**Figure 3. Ectopic S100A14 expression and knockdown in lentivirus-mediated stable cells.**

Whole cell lysate and total RNA pool were collected from TOV112D (A, Left : transfected with empty clone #4, #5 or *S100A14* clone #6, #8), YDOV-151 (A, Right : transfected with empty clone #4, #5 or *S100A14* clone #6, #10), SNU840 (B, Left: transfected with empty clone #7, #8 or *S100A14* shRNA sequence #2, #5), or OVCA429 (B, Right : transfected with empty clone #3, #4 or *S100A14* shRNA sequence #2, #5) stable cells. Both shRNA of S100A14 were each other's difference sequence. Expression of S100A14 protein was analyzed by immunoblotting (upper panels) and mRNA level was measured by real-time PCR (lower panels). GAPDH was included as an internal loading control.

**7. The role of S100A14 in cell proliferation and colony formation**

We analyzed the effect of S100A14 overexpression on cell proliferation of TOV112D and YDOV-151 stable cells using WST-1 assay (short time) and colony formation assay (long time). The cell growth assay revealed that cell growth rate in both of S100A14-transfected cells was significantly higher than empty vector-expressed cells (Fig. 4A). Similar results were also observed in colony formation assay (Fig 4B). The cell growth rate of knockdown of S100A14 in SNU840 or OVCA429 stable cells were not significantly altered in WST-1 assay (Fig. 4C). But, in colony forming-assay, knockdown of S100A14 in SNU840 and OVCA429 stable cells significantly decreased colony formation efficacy compared with sh-control group (Fig. 4D).

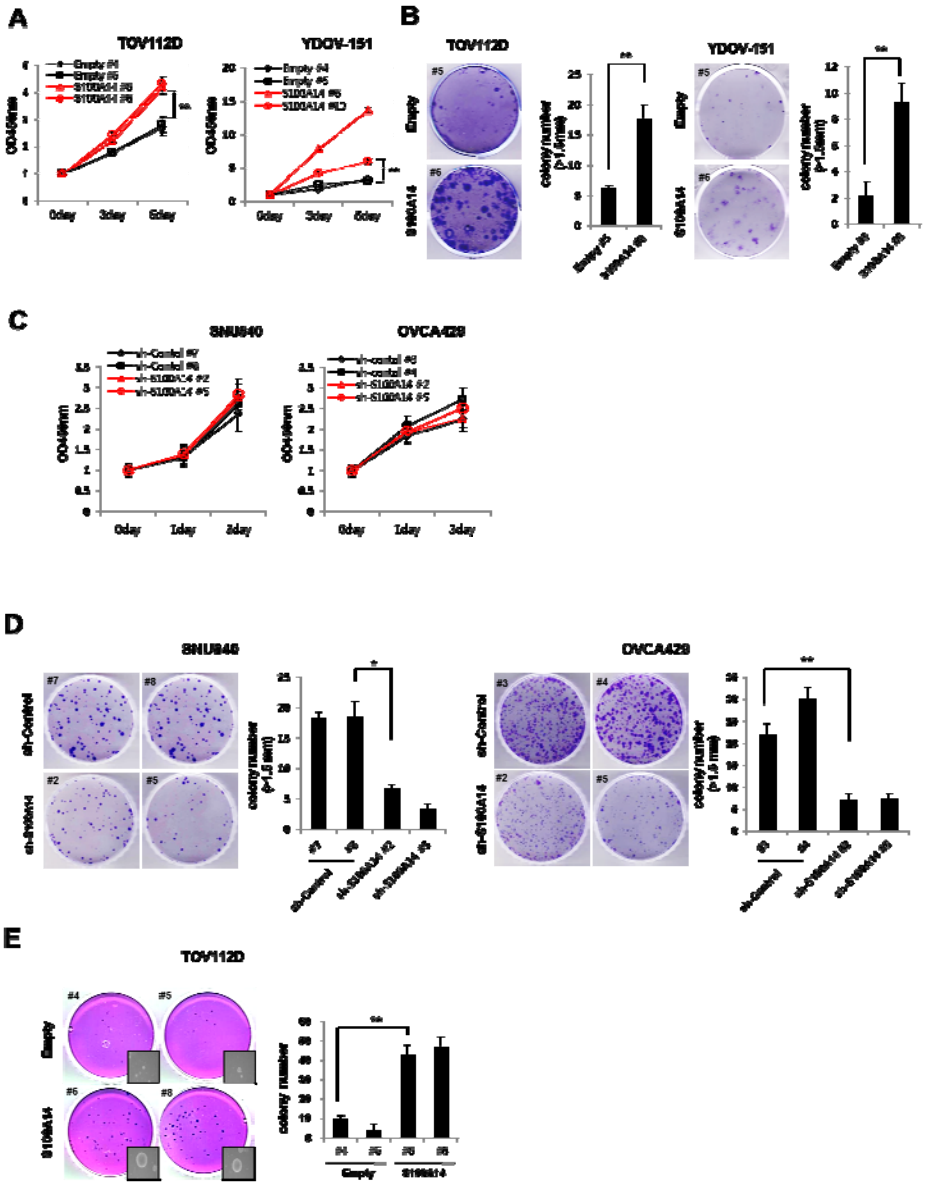
A
TOV112D
YDOV-151
B
TOV112D
YDOV-151
C
SNU840
OVCA429
D
SNU840
OVCA429
E
TOV112D

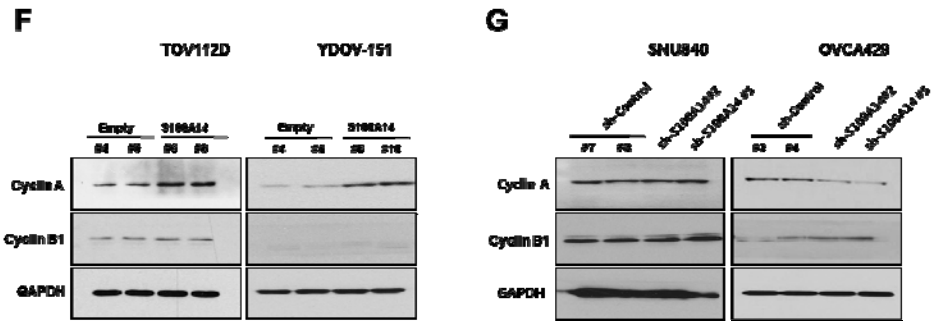


**Figure 4. S100A14 increases cell proliferation and tumorigenesis.**

A) Cell proliferation was determined by WST-1 assay. Cell proliferation curves of TOV112D and YDOV-151 stable cells at the indicated times. Error bars represent ± SD of triplicated experiments. B) Colony-forming assay, the clonogenic assay was performed with TOV112D and YDOV-151 stable cells for 3 weeks. Left panel showed the representative images, and right panel showed the quantification of colonies. Error bars represent ±SD of triplicated experiments. C) Cell proliferation was determined by WST-1 assay. Cell proliferation curves of SNU840 and OVCA429 stable cells at the indicated times. Error bars represent ± SD of triplicated experiments. D) Colony-forming assay, the clonogenic assay was performed with SNU840 and OVCA429 stable cells for 3 weeks. Left panel showed the representative images, and right panel showed the quantification of colonies. Error bars represent ±SD of triplicated experiments. E) Soft-agar colony formation assay was performed with TOV112D stable cells. Left panel showed the representative picture, and right panel showed the quantification of colonies. Error bars represent ± SD of triplicated experiments. F, G) Cyclin A, B1 expression in S100A14-tranfected and -knockdown cells. Whole cell lysate were collected from TOV112D, YDOV-151, SNU840 and OVCA429 stable cells. Cyclin A, B1 protein levels was assessed by western blotting. GAPDH was included as an internal loading control. An asterisk (*) indicates a $p$-value < 0.05, and a double asterisk (**), a

*p*-value < 0.01.

We next performed soft agar colony assay for tumorigenesis. The number of colony in S100A14-transfected cells in TOV112D was significantly higher than empty vector-expressed cells (Fig. 4E). Because previous studies provided the evidence that cyclin A was related to tumorigenesis,[20] we investigated the protein expression of cyclin A in S100A14-tranfected and -knockdown cells by using western blotting. Consistent with the changes in cell growth, the protein expression of cyclin A increased in S100A14-overexpressed TOV112D and YDOV-151 stable cells while it decreased in S100A14-knockdown OVCA429 stable cells (Fig. 4F and 4G). However, there was no difference of Cycin A expression in S100A14-knockdown SNU840 stable cells.

**8. S100A14 affects cell migration and invasion**

To investigate whether S100A14 plays a role in the migration capability of EOC cells, we conducted wound healing assay for cell migration and found that overexpression of S100A14 increased motility of TOV112D stable cells compared with empty vector-expressed cells (Fig. 5A). In contrast, shRNA-mediated S100A14 knockdown inhibited the cell motility in SNU840 stable cells (Fig. 5B). To evaluate whether S100A14 could also enhance the invasion ability of EOC cells, Matrigel invasion assay was performed. When we tested the basic capability of cell invasion in EOC cells, SNU840 and OVCA429 which have the higher level of endogenous S100A14 showed the

significantly higher invasion potential than TOV112D and YDOV-151cells with lower endogenous S100A14 (Fig. 5C). To further confirm the role of S100A14 in cell invasion, we evaluated the invasion potential in TOV112D, YDOV-151, and OVCA429 stable cells. S100A14 overexpression in TOV112D (*S100A14* #8) and YDOV-151 (*S100A14* #6, #10) stable cells led to increased invasion compared to empty vector-expressed cells (Fig. 5D). In contrast, S100A14 knockdown in OVCA429 (sh-*S100A14* #2, #5) stable cells led to decreased invasion (Fig. 5E). To explore the molecular mechanism of S100A14 promoting cell migration and invasion, we characterized the expression of some metastatic related genes by RT-PCR analysis (Fig. 5F). Interestingly, among the MMPs that were detected, MMP1 and MMP9 expressions were dramatically induced in the S100A14-overexpression in TOV112D stable cells. In contrast, expression of MMP2 was not significantly altered. Real-time PCR analysis further confirmed the dramatic increase of MMP1 and MMP9 expression (Fig. 5F). Taken together, these results demonstrate that S100A14 plays an important role in cell motility and invasiveness.

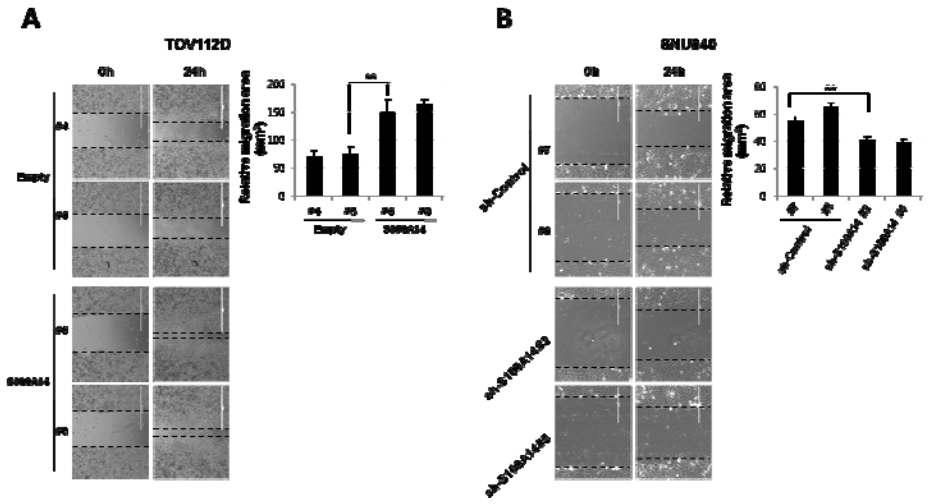

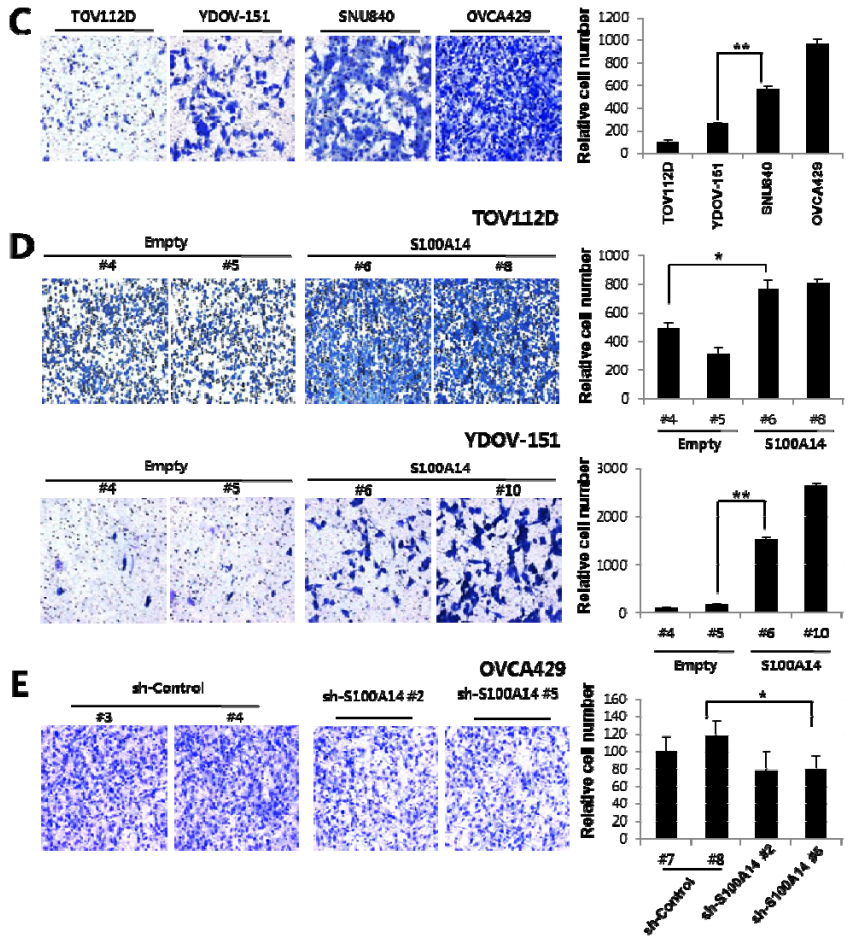
C
TOV112D
YDOV-151
SNU840
OVCA429
Relative cell number
D
TOV112D
Empty
S100A14
#4
#5
#6
#8
YDOV-151
#10
E
OVCA429
sh-Control
sh-S100A14 #2
sh-S100A14 #5
#3
#7

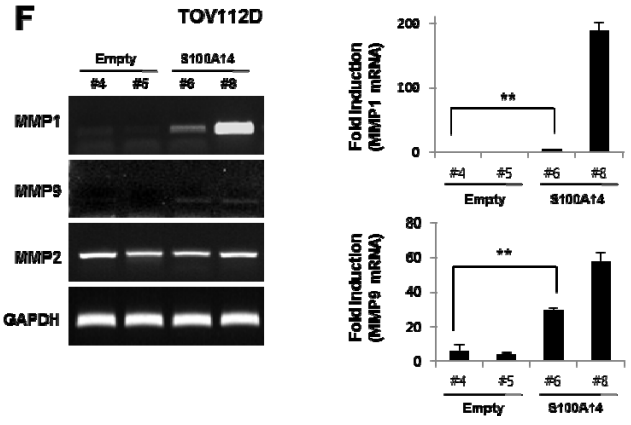
F
TOV112D
Empty
S100A14
MMP1
MMP9
MMP2
GAPDH
Fold Induction (MMP1 mRNA)
Fold Induction (MMP9 mRNA)

**Figure 5. S100A14 promotes cell migration and invasion.**

Cell migration analyses of TOV112D (A) and SNU 840 (B) cells by wound healing assay. Left panel: Representative images of migrations assays. Right panel: Quantitative results of migration experiments. Results are presented as the relative migration area. Cell invasion analysis of non-treated EOC cells (C), or TOV112D (D), YDOV-151 (D) and OVCA429 (E) stable cells using Matrigel invasion assay. Left panel: Representative figures of cell invasion. Right panel: Quantitative results of invasion experiments. Results are presented as the relative numbers of invading cells. Cells were counted in 4 randomly selected fields. (F) Expression of matrix metalloproteinase (MMP)1, MMP9 and MMP2 were assessed by using RT-PCR (Left) and real-time PCR (Right) in TOV112D stable cells. Expression of GAPDH was included as internal loading control. An asterisk (*) indicates a *p*-value < 0.05, and a double asterisk (**), a *p*-value < 0.01.

## 9. S100A14 promotes malignant phenotype in EOC cells through Akt signaling pathway

To verify the correlation of S100A14 and Akt phosphorylation in EOC, we conducted western blotting using specific antibody, S100A14 and phospho-Akt$^{S473}$ (pAkt) in whole cell lysates that were taken from TOV112D, SNU840, OVCA429, YDOV-105, YDOV-151, YDOV-13, and YDOV-139 cells. TOV112D and YDOV151 cells which lack endogenous S100A14 expression showed the lower level of pAkt compared to the cells with higher endogenous S100A14 expression (Fig. 6A). And then, to confirm the relations between S100A14 and pAkt, we conducted western blotting in whole cell lysate from

S100A14-overexpressed and shRNA-knockdown cells. S100A14 overexpression in TOV112D (*S100A14* #6, #8) and YDOV-151 (*S100A14* #6, #10) cells led to increased level of pAkt (Fig. 6B), while S100A14 knockdown in SNU840 (sh-*S100A14* #2, #5) and OVCA429 (sh-*S100A14* #2, #5) cells led to decreased pAkt (Fig. 6C). However, there was no detectable change in either pErk or Erk expression after S100A14 transduction. These data suggest that S100A14 potentially modulated the activity of Akt.

To define the role of Akt in S100A14-modulated cell proliferation and invasion, we treated TOV112D (*S100A14* #6, #8) cells with PI3K (Akt upstream kinase) inhibitor wortmannin or Akt inhibitor MK-2206 and evaluated the effect on cell proliferation and invasion. First, we confirmed specificity of the inhibitors by western blot analysis (Fig. 6D). Increased pAkt levels in S100A14-overexpression cells were significantly decreased by wortmannin or MK-2206. Next, we found that treatment with wortmannin or MK-2206 significantly decreased S100A14-enhaned cell proliferation and invasion using colony forming assay and invasion assay (Fig 6E and 6F). Taken together, these data demonstrate that S100A14 controls cell proliferation and invasive potential through regulation of PI3K/Akt pathway.

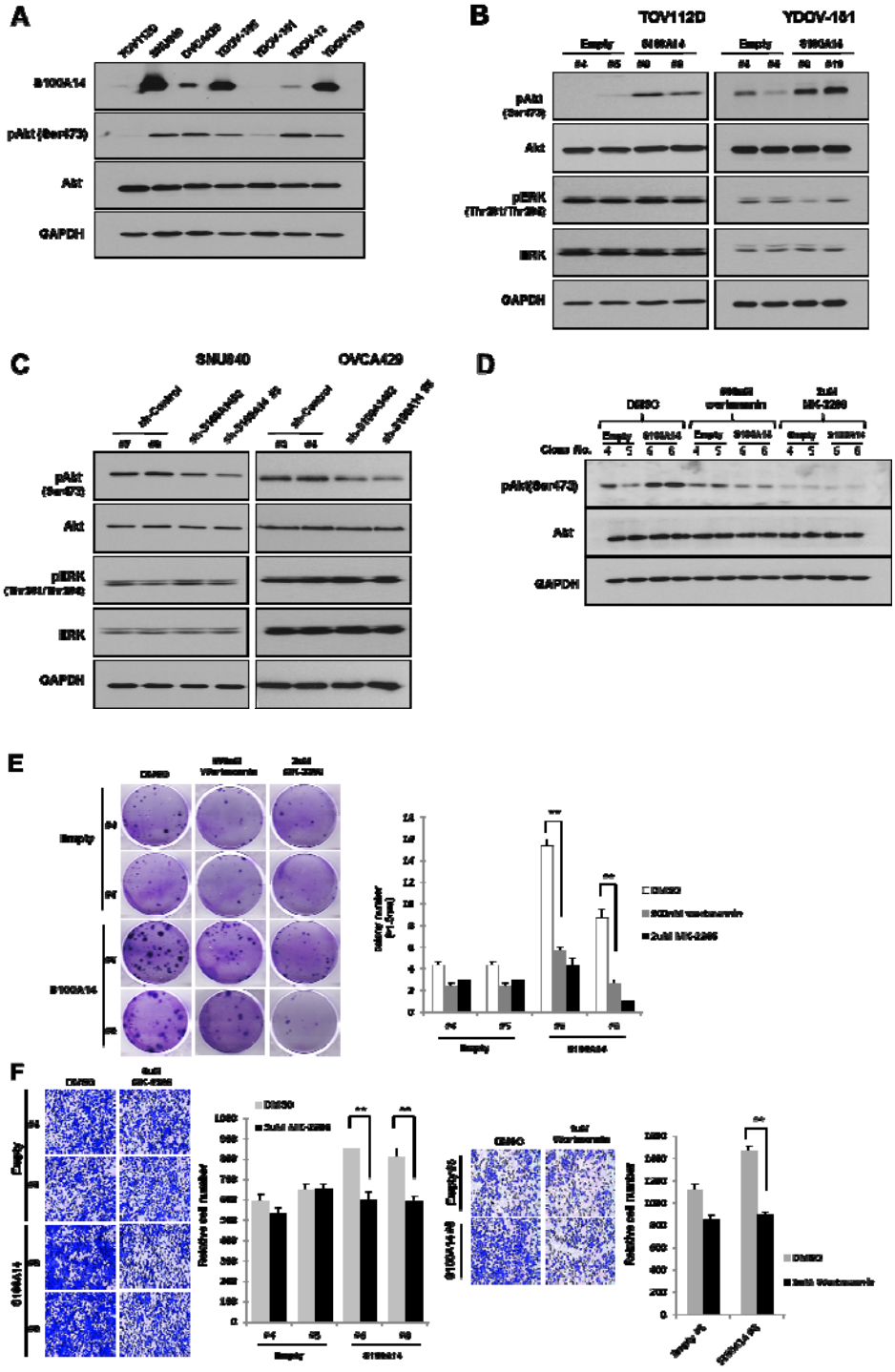
A
B
TOV112D
YDOV-151
Empty
S100A14
pAkt (Ser473)
Akt
pERK (Thr201/Thr204)
ERK
GAPDH
C
SNU840
OVCA429
shControl
shS100A14 #5
shS100A14 #6
D
DMSO
Wortmannin
MK-2206
Clone No.
E
Empty
S100A14
Relative cell number
F

**Figure 6. S100A14 controls oncogenic phenotypes of EOC cells through PI3K/Akt pathway.**

A) The protein expression of S100A14, pAkt (ser478), and Akt was determined by western blot in non-transfected EOC cells. Expression of pERK (thr201/204) and ERK were assessed by western blot in TOV112D and YDOV-151 stable cells (B), and SNU840 and OVCA429 stable cells (C). GAPDH was included as an internal loading control. D) Western blot analysis of pAkt inhibition in TOV112D stable cell treated with wortmannin, MK-2206 or control (DMSO) for 8h. E) Colony-forming assay, the clonogenic assay was performed with TOV112D stable cells for 3 weeks in the presence of wortmannin, MK-2206 or control (DMSO). Left panel showed the representative images, and right panel showed the quantification of colonies. Error bars represent ±SD of triplicated experiments. F) Cell invasion analysis of TOV112D stable cells with wortmannin, MK-2206 or control (DMSO). All drugs were applied to the upper chamber. Left panel: Representative figures of cell invasion. Right panel: Quantitative results of invasion experiments. Results are presented as the relative numbers of invading cells. Cells were counted in 6 randomly selected fields. An asterisk (*) indicates a $p$-value < 0.05, and a double asterisk (**), a $p$-value < 0.01.

## IV. DISCUSSION

Carcinogenesis is the result of a series of molecular changes that have occurred in a cell. However, little is known of the molecular changes that are associated with carcinogenesis of invasive ovarian cancer. To identify genes which could potentially be useful as novel diagnostic and/or therapeutic markers for EOC, we evaluated the gene expression patterns of 6 EOC cell lines which were established and characterized in our institute by cDNA microarray and compared their genetic fingerprints to those of 4 HOSE cells. Only cancer

cell lines derived from epithelial ovarian cancer, which is the most common type of ovarian cancer, were included to limit the complexity of gene expression analysis.

In microarray analysis, a total of 859 probe sets were found to be significantly overexpressed in EOC cell lines when compared to HOSE cells, while 1116 probe sets were found overexpressed in HOSE cells. Because genes that may not show striking overexpression of transcripts may have significant serum levels, using too stringent microarray criteria for choosing candidate genes may exclude these candidates. Therefore, in this study, the average change in expression level between the two groups was at least 2-fold. A large number of genes overexpressed in ovarian cancers were associated with epithelia. This might reflect the epithelial origin of these tumors. Several of the genes identified in this study, including *Kallikrein6/7, CLDN3/7, TACSTD1* (*Ep-CAM*), and *Prostasin*, have been previously shown to be differentially expressed in ovarian carcinomas,[21-25] providing strong experimental support for the microarray analysis. The present results thus further confirm their presence and support their role in ovarian carcinogenesis. The known function of some of these genes may provide insights in the biology of EOC. However, comparing our microarray data to previous studies on ovarian cancer-related genes revealed only a minor degree of overlap, indicating that the extent of gene expression differences far exceeds the number of genes identified in this or other previous studies.

We also carried out a comparative proteome study using MALDI-TOF and PMF to identify differentially expressed proteins between EOC cell lines and HOSE cells. Proteomics is the study of global protein expression patterns in a cell, tissue, or organism. A major advantage of proteome studies is the possibility of analyzing post-translational modifications; a number of gene products can arise from a single gene due to various post-translational modifications, resulting in a substantially increased complexity of proteins

compared to RNA transcripts. Several proteins up-regulated in this proteomic analysis belonged to the functional class of stress response and chaperone proteins. Heat shock protein (HSP) 27 has been related to cell growth and motility, and high HSP27 expression has been associated with poor prognosis in various types of malignancies including ovarian cancer.[26,27] We also identified Annexin A4 and Annexin1, which are members of the annexin family (I-XIII). These proteins are calcium-dependent phospholipid-binding proteins, and play a role in the regulation of cellular growth, cell to cell adhesion process, calcium flux, and vesicle trafficking.[28] Other up-regulated proteins identified in the current study included Enolase 1, ER-60 protein, and Ubiquinol-cytochrome c reductase core I protein.

Highly expressed genes in our microarray analysis included *S100A14*, whose expression level was 6.29-fold greater than HOSE cells. The S100 proteins are low-molecular-weight, calcium-binding proteins comprising 20 known members each coded by a separate gene. The calcium binding of *S100* proteins is thought to be important for their functional activity.[29] Increased expression of several S100 proteins has been associated with many malignancies, and these proteins are thought to be implicated in a number of biological functions of cancer.[30-32] However, the mode of action of many S100 proteins in cancer remains to be elucidated, and the functional implications of altered S100 expression levels must be determined. Pietas and colleagues identified a new S100 member, named S100A14, by analyzing a human lung cancer cell line subtraction cDNA library.[10] They also demonstrated its overexpression in ovary, breast, and uterus tumor tissues by northern blot hybridization. Future study of the molecular mechanisms by which S100A14 affects the process of cancer is needed to determine the biological function of this novel gene.

In addition to the identification of novel diagnostic markers for ovarian cancer, a further understanding of molecular mechanisms underlying the

progression and metastasis of ovarian cancer is needed to develop effective therapeutic modalities. Among the differentially expressed genes and proteins that we have identified, we have selected S100A14 for further studies, due to their significant overexpression in all of the six EOC cell lines and potential relations with cancer cell growth and survival. Afterwards we investigated the relation between S100A14 expression and clinicopathological parameters including survival in EOC tissue specimens and studied the functional role of S100A14 using lentivirus-mediated overexpression and knockdown followed by various *in vitro* assays.

In this study S100A14 was elevated at both mRNA and protein levels in EOC cells and tissues using real-time PCR (Fig. 2A), immune blotting (Fig. 2B), and IHC analysis (Fig. 2C). In real-time PCR, 81.8% (9/11) of EOC cell lines exhibited increased *S100A14* mRNA expression compare to normal HOSE cells. By the subsequent immunohistochemical assay, the mean score of EOC (5.37, 95% CI = 5.21-5.52) was significantly higher ($P < 0.001$) than that of borderline (3.76, 95% CI = 2.44-5.09), benign (1.90, 95% CI = 0.70-3.10), and normal tissue (0.20, 95% CI = -0.13-0.54). In agreement with our study, the increased S100A14 expression has been reported in circulating tumor cells from breast and colorectal cancers.[33] We also examined whether S100A14 overexpression is a predictive marker of more aggressive behavior by correlating the IHC score to clinicopathological variables and revealed that tumors with high S100A14 expression were associated with more aggressive phenotypes of EOC such as advanced tumor stage ($P < 0.001$) and poor tumor grade ($P < 0.001$) (Table 5). Tumor grade is an important prognostic parameter for the risk stratification of EOC patients. However, tumor grading may be subjective and may produce conflicting results even among experienced pathologists. In such cases, S100A14 IHC score could serve as an additional method for supplementing the histologic grading and predicting prognosis of EOC by providing objective and quantitative measurements. In a recent report, contrary to our study, it has been

showed that loss of S100A14 expression was associated with lymph node metastasis and advanced disease stage in IHC study of 175 small intestinal adenocarcinoma patients.[34] The discrepancy maybe partially explained by the difference of antibodies applied to the staining or methods of IHC procedures, but most of all, the difference of anatomic sites. Therefore, further studies which can give additional information about the proposed role of S100A14 are strongly recommended.

It was recently proposed that ovarian cancer can be divided into two main categories designated type I and type II tumors based on their distinct pathogenesis.[35] Type I tumors are well-differentiated serous, mucinous, endometrioid, malignant Brenner, and clear cell tumors that generally exhibit slow indolent growth and Ras and Raf mutation. In contrast, type II tumors include moderately- or poorly-differentiated serous, undifferentiated, and malignant mixed mesodermal tumors with p53 mutation those are highly aggressive and present at advanced stage, when current available therapies are seldom curative.[36] To compare S100A14 expression according to these molecular subtypes, we performed subgroup analysis of IHC results in type I and type II tumors. S100A14 protein expression was significantly stronger in type II tumors (IHC score = 5.42, n=52) in comparison with type I tumors (IHC score = 4.85, n=19) ($P < 0.001$). When we consider that type II tumors are more aggressive than type I tumors and constitute approximately 75% of ovarian cancer,[37] it is reasonable to focus on type II tumors for the identification of biomarkers in the future.

One of our most notable finding is that S100A14 overexpression in EOC predicts a shorter survival time. By univariate analysis of Cox hazard model, S100A14+, advanced tumor stage, poor tumor grade, and serous cell types were associated with increased risk of recurrence from EOC. Moreover, S100A14+ and advanced tumor stage was independent prognostic factors for both disease-free and overall survival on multivariate analysis (Table 6). To our

knowledge, the observation that S100A14 expression increases in EOC and is related to poor survival is described for the first time here. Taken together, these results suggest that S100A14 might play an important role in the pathogenesis of EOC.

Increasing evidence showed the critical role of S100 family in cell growth, invasion, and cancer metastasis. Therefore, based on our results from analysis of clinical specimens, we investigated the potential roles of S100A14 in EOC. Lentiviral vector mediated overexpression of S100A14 resulted in the significant increases of proliferation and tumorigenesis capacity, and conversely, shRNA mediated knockdown of S100A14 led to suppression of these phenotypes (Fig. 4A-E). Moreover, modulation of Cyclin A was shown to underlie the regulation of cell proliferation seen in EOC cells following S100A14 overexpression or knockdown (Fig. 4F and G). Taken together, these findings suggest that S100A14 could contribute to the development and progression of EOC. In addition to increased proliferation after S100A14 transduction, we found that S100A14 can affect the migration and invasion capacity of EOC cells (Fig. 5A-F). Recently, it has been reported that S100A14 promoted cell motility and invasiveness by regulating the expression and function of MMP2 in a p53-dependent manner in esophageal squamous cell carcinoma cells.[38] Similarly, our study showed that MMP1 and MMP9 expression was induced in S100A14-overexpressed TOV112D stable cells (Fig. 5F). Overexpression of MMP1 has been shown to be associated with progression of oral dysplasia to cancer.[39] Taken together, it can be speculated that S100A14 modulates the invasive phenotype of EOC cells and this regulation might be associated with the modulation of MMP1, which is known to be involved in invasion and metastasis. However S100A14 has also been shown to reduce cell invasion as retroviral vector mediated overexpression of S100A14 resulted in significant decrease in the invasive potential of oral squamous cell carcinomas cells.[12] To date, the molecular mechanism by which

S100A14 regulates cell proliferation and/or invasion remain elusive.

To determine the underlying mechanism by which S100A14 confers a growth and invasion advantage to EOC cells, we next investigated whether Akt or Erk signaling pathway is compromised upon S100A14 overexpression or knockdown. Interestingly, we found that the expression of pAkt is obviously increased after S100A14 gene overexpression in TOV112D and YDOV-151 stable cells (Fig 6B). Conversely, S100A14 knockdown decreased pAkt expression in SNU840 and OVCA429 stable cells (Fig. 6C). However, there was no detectable change in either pErk or Erk expression after S100A14 modulation (Fig 6B and C). Furthermore, we showed that PI3K (wortmannin ) or Akt inhibitor (MK-2206) treatment inhibited Akt activation (Fig. 6D), cell proliferation (Fig. 6E), and cell invasion (Fig. 6F) in TOV112D or YDOV-151 stable cells. Taken together, our data suggest that S100A14 mediates the malignant phenotype of EOC cells through the activation of Akt. Taken together, our data suggest that S100A14 mediates the malignant phenotype of EOC cells possibly through the activation of Akt.

## V. CONCLUSION

In summary, this is the first report, to our knowledge, to show that the protein expressions of S100A14 increase from normal ovarian epitheliums throughout benign and borderline ovarian tumors to EOC tissues. We also showed important correlations between S100A14 expression and clinicopathogical parameters including survival that might indicate potentially clinically useful results. In addition, S100A14 promotes cell motility and invasiveness by regulating the expression and function of pAkt. Given its important role in ovarian carcinogenesis, S100A14 may have significant potential in therapeutic applications.

**REFERENCES**


1. Jemal A, Siegel R, Ward E, Murray T, Xu J, Thun MJ. Cancer statistics, 2007. CA Cancer J Clin 2007;57:43-66.
2. Auersperg N, Wong AS, Choi KC, Kang SK, Leung PC. Ovarian surface epithelium: biology, endocrinology, and pathology. Endocr Rev 2001;22:255-88.
3. Donato R. S100: a multigenic family of calcium-modulated proteins of the EF-hand type with intracellular and extracellular functional roles. Int J Biochem Cell Biol 2001;33:637-68.
4. Donato R. Intracellular and extracellular roles of S100 proteins. Microsc Res Tech 2003;60:540-51.
5. Marenholz I, Heizmann CW, Fritz G. S100 proteins in mouse and man: from evolution to function and pathology (including an update of the nomenclature). Biochem Biophys Res Commun 2004;322:1111-22.
6. Salama I, Malone PS, Mihaimeed F, Jones JL. A review of the S100 proteins in cancer. Eur J Surg Oncol 2008;34:357-64.
7. Saleem M, Kweon MH, Johnson JJ, Adhami VM, Elcheva I, Khan N, et al. S100A4 accelerates tumorigenesis and invasion of human prostate cancer through the transcriptional regulation of matrix metalloproteinase 9. Proc Natl Acad Sci U S A 2006;103:14825-30.
8. Whiteman HJ, Weeks ME, Dowen SE, Barry S, Timms JF, Lemoine NR, et al. The role of S100P in the invasion of pancreatic cancer cells is mediated through cytoskeletal changes and regulation of cathepsin D. Cancer Res 2007;67:8633-42.
9. Bulk E, Sargin B, Krug U, Hascher A, Jun Y, Knop M, et al. S100A2 induces metastasis in non-small cell lung cancer. Clin Cancer Res 2009;15:22-9.
10. Pietas A, Schluns K, Marenholz I, Schafer BW, Heizmann CW, Petersen I. Molecular cloning and characterization of the human

S100A14 gene encoding a novel member of the S100 family. Genomics 2002;79:513-22.

11. Yao R, Lopez-Beltran A, Maclennan GT, Montironi R, Eble JN, Cheng L. Expression of S100 protein family members in the pathogenesis of bladder tumors. Anticancer Res 2007;27:3051-8.
12. Sapkota D, Bruland O, Costea DE, Haugen H, Vasstrand EN, Ibrahim SO. S100A14 regulates the invasive potential of oral squamous cell carcinoma derived cell-lines in vitro by modulating expression of matrix metalloproteinases, MMP1 and MMP9. Eur J Cancer 2011;47:600-10.
13. Cho H, Kang ES, Hong SW, Oh YJ, Choi SM, Kim SW, et al. Genomic and proteomic characterization of YDOV-157, a newly established human epithelial ovarian cancer cell line. Mol Cell Biochem 2008;319:189-201.
14. Cho H, Lim BJ, Kang ES, Choi JS, Kim JH. Molecular characterization of a new ovarian cancer cell line, YDOV-151, established from mucinous cystadenocarcinoma. Tohoku J Exp Med 2009;218:129-39.
15. Eberwine J, Yeh H, Miyashiro K, Cao Y, Nair S, Finnell R, et al. Analysis of gene expression in single live neurons. Proc Natl Acad Sci U S A 1992;89:3010-4.
16. Irizarry RA, Bolstad BM, Collin F, Cope LM, Hobbs B, Speed TP. Summaries of Affymetrix GeneChip probe level data. Nucleic Acids Res 2003;31:e15.
17. Therasse P, Arbuck SG, Eisenhauer EA, Wanders J, Kaplan RS, Rubinstein L, et al. New guidelines to evaluate the response to treatment in solid tumors. European Organization for Research and Treatment of Cancer, National Cancer Institute of the United States, National Cancer Institute of Canada. J Natl Cancer Inst 2000;92:205-16.

18. Shibusa T, Shijubo N, Abe S. Tumor angiogenesis and vascular endothelial growth factor expression in stage I lung adenocarcinoma. Clin Cancer Res 1998;4:1483-7.
19. Livak KJ, Schmittgen TD. Analysis of relative gene expression data using real-time quantitative PCR and the 2(-Delta Delta C(T)) Method. Methods 2001;25:402-8.
20. Katabami M, Donninger H, Hommura F, Leaner VD, Kinoshita I, Chick JF, et al. Cyclin A is a c-Jun target gene and is necessary for c-Jun-induced anchorage-independent growth in RAT1a cells. J Biol Chem 2005;280:16728-38.
21. Kim JH, Herlyn D, Wong KK, Park DC, Schorge JO, Lu KH, et al. Identification of epithelial cell adhesion molecule autoantibody in patients with ovarian cancer. Clin Cancer Res 2003;9:4782-91.
22. Mok SC, Chao J, Skates S, Wong K, Yiu GK, Muto MG, et al. Prostasin, a potential serum marker for ovarian cancer: identification through microarray technology. J Natl Cancer Inst 2001;93:1458-64.
23. Paliouras M, Borgono C, Diamandis EP. Human tissue kallikreins: the cancer biomarker family. Cancer Lett 2007;249:61-79.
24. Rangel LB, Agarwal R, D'Souza T, Pizer ES, Alo PL, Lancaster WD, et al. Tight junction proteins claudin-3 and claudin-4 are frequently overexpressed in ovarian cancer but not in ovarian cystadenomas. Clin Cancer Res 2003;9:2567-75.
25. Tassi RA, Bignotti E, Falchetti M, Ravanini M, Calza S, Ravaggi A, et al. Claudin-7 expression in human epithelial ovarian cancer. Int J Gynecol Cancer 2008.
26. Storm FK, Mahvi DM, Gilchrist KW. Heat shock protein 27 overexpression in breast cancer lymph node metastasis. Ann Surg Oncol 1996;3:570-3.
27. Arts HJ, Hollema H, Lemstra W, Willemse PH, De Vries EG,

Kampinga HH, et al. Heat-shock-protein-27 (hsp27) expression in ovarian carcinoma: relation in response to chemotherapy and prognosis. Int J Cancer 1999;84:234-8.

28. Moss SE, Morgan RO. The annexins. Genome Biol 2004;5:219.
29. Donato R. Functional roles of S100 proteins, calcium-binding proteins of the EF-hand type. Biochim Biophys Acta 1999;1450:191-231.
30. Ji J, Zhao L, Wang X, Zhou C, Ding F, Su L, et al. Differential expression of S100 gene family in human esophageal squamous cell carcinoma. J Cancer Res Clin Oncol 2004;130:480-6.
31. Perez D, Demartines N, Meier K, Clavien PA, Jungbluth A, Jaeger D. Protein S100 as prognostic marker for gastrointestinal stromal tumors: a clinicopathological risk factor analysis. J Invest Surg 2007;20:181-6.
32. Zou M, Al-Baradie RS, Al-Hindi H, Farid NR, Shi Y. S100A4 (Mts1) gene overexpression is associated with invasion and metastasis of papillary thyroid carcinoma. Br J Cancer 2005;93:1277-84.
33. Smirnov DA, Zweitzig DR, Foulk BW, Miller MC, Doyle GV, Pienta KJ, et al. Global gene expression profiling of circulating tumor cells. Cancer Res 2005;65:4993-7.
34. Kim G, Chung JY, Jun SY, Eom DW, Bae YK, Jang KT, et al. Loss of S100A14 expression is associated with the progression of adenocarcinomas of the small intestine. Pathobiology 2013;80:95-101.
35. Shih Ie M, Kurman RJ. Ovarian tumorigenesis: a proposed model based on morphological and molecular genetic analysis. Am J Pathol 2004;164:1511-8.
36. Kurman RJ, Visvanathan K, Roden R, Wu TC, Shih Ie M. Early detection and treatment of ovarian cancer: shifting from early stage to minimal volume of disease based on a new model of carcinogenesis. Am J Obstet Gynecol 2008;198:351-6.
37. Kurman RJ, Shih Ie M. The origin and pathogenesis of epithelial

ovarian cancer: a proposed unifying theory. Am J Surg Pathol 2010;34:433-43.

38. Chen H, Yuan Y, Zhang C, Luo A, Ding F, Ma J, et al. Involvement of S100A14 protein in cell invasion by affecting expression and function of matrix metalloproteinase (MMP)-2 via p53-dependent transcriptional regulation. J Biol Chem 2012;287:17109-19.

39. Jordan RC, Macabeo-Ong M, Shiboski CH, Dekker N, Ginzinger DG, Wong DT, et al. Overexpression of matrix metalloproteinase-1 and -9 mRNA is associated with progression of oral dysplasia to cancer. Clin Cancer Res 2004;10:6460-5.

< ABSTRACT(IN KOREAN)>

## S100A14는 상피성 난소암에서 AKT를 매개로 하는 종양 형성 능력이 있으며 나쁜 예후를 예측한다

<지도교수 김재훈>

연세대학교 대학원 의학과

조한별

**목적:** 본 연구의 목적은 상피성 난소암에서 과발현되는 유전자 및 단백질을 발굴하고, 이를 바탕으로 새로운 진단 및 예후 표지자를 개발하는 것이다. 또한 새로운 표지자 후보인 S100A14의 난소암 발생 과정에서의 역할을 알아 보고자 하였다.

**방법:** 새로운 상피성 난소암 세포주 6개를 확립하고 특성화 하였으며, microarray 결과의 유효성 검증을 위해 104개의 난소암 조직에서 S100A14 mRNA 및 단백질 발현을 측정하였다. 또한 lentivirus와 shRNA 기법을 이용하여 S100A14 과발현 또는 무력화 세포를 확립하고 S100A14의 난소암 암화 과정에의 역할을 연구 하였다.

**결과:** Illumina microarray 결과 난소암에서 과발현된 859개의 유전자를 확보하고 PCR, western blotting, 면역화학염색법을 이용하여 S100A14 발현이 난소암 세포와 조직에서 증가되어 있음을 확인 하였다. S100A14 단백질 발현은 병기, 분화도와 같은 예후 인자와 양의 상관관계를 보였으며 ($P<0.001$), 다변량 생존분석에서 S100A14 발현($P=0.029$)은 암병기($P=0.024$)와 함께 난소암 생존의 독립적 예후 인자였다. 난소암 세포주를 이용한 기능 연구 결과 S100A14가 세포 증식, 종양 형성, 세포 이동 및 침습에 AKT 신호전달경로를 매개하여 중요한 역할을 하고 있음을 확인 하였다.

**결론:** 본 연구는 S100A14가 난소암의 암화과정에 중요한 역할을 하고 있으며 난소암 표적치료의 새로운 표지자로서의 가능성이 있음을 보여주었다.

---

핵심되는 말 : 난소암; 암표지자; S100A14; lentivirus; shRNA